

# Convergence of Regular Spiking and Intrinsically Bursting Izhikevich Neuron Models as a Function of Discretization Time with Euler Method

Harish Gunasekaran<sup>a,1</sup>, Giacomo Spigler<sup>b,1</sup>, Alberto Mazzoni<sup>b</sup>, Enrico Cataldo<sup>c</sup>, Calogero Maria Oddo<sup>b,\*</sup>

<sup>a</sup>*University of Pisa, Pisa, Italy*

<sup>b</sup>*The Biorobotics Institute, Scuola Superiore Sant'Anna, Pisa, Italy*

<sup>c</sup>*Physics Department, University of Pisa, Pisa, Italy*

---

## Abstract

This study investigates the trade-off between computational efficiency and accuracy of Izhikevich neuron models by numerically quantifying their convergence to provide design guidelines in choosing the limit time steps during a discretization procedure. This is important for bionic engineering and neuro-robotic applications where the use of embedded computational resources requires the introduction of optimality criteria. Specifically, the regular spiking (RS) and intrinsically bursting (IB) Izhikevich neuron models are evaluated with step inputs of various amplitudes. We analyze the convergence of spike sequences generated under different discretization time steps ( $10\mu s$  to  $10ms$ ), with respect to an ideal reference spike sequence approximated with a discretization time step of  $1\mu s$ . The differences between the ideal reference and the computed spike sequences were quantified by Victor-Purpura (VPd) and van Rossum (VRd) distances. For each distance, we found two limit discretization times ( $dt_1$  and  $dt_2$ ), as a function of the applied input and thus firing rate, beyond which the convergence is lost for each neuron model.

*Keywords:* Convergence, Izhikevich Neuron Model, Discretization, Euler method, Victor-Purpura Distance, van Rossum Distance, CUSUM

---

\*Corresponding author

*Email address:* calogero.oddo@santannapisa.it (Calogero Maria Oddo)

<sup>1</sup>These authors contributed equally to this work

## 1. Introduction

Neuromorphic electronic systems mimic structures and features of the biological nervous system and form the basis for building bionic artifacts. The level of mimicking could be either physical or only functional. That is, the neuronal components such as neurons, synapses and their learning mechanisms could be implemented via the physics of the system (hard neuromorphic approach) or on existing computer architectures (soft neuromorphic approach) [1]. Though the former enjoys the advantage of an optimized design, the latter is much more flexible and has a shorter design time. Further, the power consumption of the soft approach can be minimized to some extent by choosing artificial neuron models with low computational requirements. A key challenge in choosing such models lies in the trade-off between computational efficiency and accuracy of the implementation. This is especially important in bioengineering and robotic applications where the use of embedded systems limits the amount of computation that can be performed in real-time.

In recent years the Izhikevich spiking neuron model has been commonly used to reproduce the dynamics of different neuron types [2, 3]. This artificial neuron model is particularly suitable for real time implementation using a microprocessor or FPGA due to its good trade-off between low computational requirements and biological plausibility [4, 1, 5, 6]. Still, like most models of artificial neurons, it is sensitive to the discretization time step  $dt$  used, especially when the Euler method is adopted to solve the differential equations describing the model. Figure 1 shows an example of the different degrees of convergence of the Izhikevich neuron model when simulated with different discretization time steps  $dt$  and different input values. As an example, it can be intuitively observed that a discretization time step of  $dt = 1ms$  results in a significant variation from the ideal spike train, though the dynamics are partially preserved. However, higher discretization time steps are found to affect the dynamics of the model in a more drastic way that then impedes its use (see for example  $dt = 5ms$  in 1). Nonetheless, while larger discretization steps inevitably lead to a degree of error in the simulation of the model dynamics, they also result in lower computational requirements, as fewer updates per second are needed. The choice of an optimal time step for the discretization process is thus the result of a trade-off between the accuracy of the generated spike trains and the computational load.

Previous studies have already investigated the numerical stability and accuracy of various neuron models [7, 8, 9, 10]. Of particular interest are Long et al.

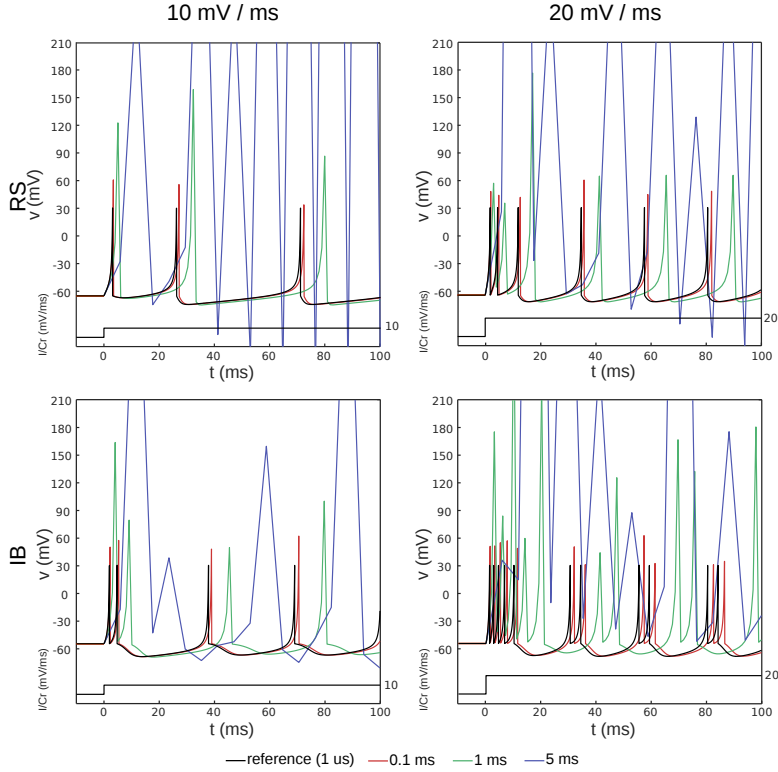


Figure 1: The membrane potential variable  $v$  is plotted within a window of  $T = 100ms$  to show the effect of the discretization time step ( $dt$ ) on the converge of a regular spiking (RS; top) and intrinsically bursting (IB; bottom) Izhikevich spiking neuron model. The left column shows simulations with an input value  $\frac{I}{C_r}$  of  $10mV/ms$ , while the right one used an input of  $20mV/ms$ . Three different values of the time step are used ( $0.1ms$ ,  $1ms$  and  $5ms$ ), along with an ideal reference trace computed using  $dt = 1\mu s$ . Note that the value of the membrane potential  $v$  can exceed the threshold of  $30mV$  if the single update that leads to its crossing is very large, for example when using large time steps.

[8] and Skocik and Long [10]. Long and colleagues addressed the convergence issues of various spiking neuron models including the Izhikevich neuron model by quantifying convergence and accuracy using the  $L^2$  norm. Skocik and Long then later compared the computational requirements of three different artificial neuron models, Hodgkin-Huxley, Izhikevich and leaky Integrate-and-Fire for attaining an accurate numerical solution of their differential equations using different methods (Euler, 4<sup>th</sup> order Runge-Kutta and exponential Euler). Contrary to the present study, however, the authors measured the errors in the resulting firing frequency and deviation from the ideal membrane voltage dynamics, rather than investigating potential trade-offs of slight decreases in the accuracy of timing of

the spike trains in exchange for gains in computational efficiency, as instead we propose here.

In this paper, we analyze the convergence of the Izhikevich neuron model using the Victor-Purpura (VPd) and van Rossum (VRd) distances between spike trains generated using multiple time steps and the ideal reference spike train. To further show the generality of the proposed approach, we report results for two sets of parameters of the Izhikevich neuron model, producing regular spiking (RS) and intrinsically bursting (IB) dynamics.

## 2. Materials and Methods

### 2.1. Izhikevich Spiking Neuron Model

Several models have been proposed to simulate the spiking dynamics of biological neurons. The first and most famous is the Hodgkin-Huxley (HH) model, that was proposed in 1952 [11] and models the role of ionic mechanisms on the genesis and propagation of action potentials. The model has been studied extensively using analytical and computational approaches [12].

A line of this research involved a qualitative analysis of the mathematical structure of the HH model. The reduction of the mathematical complexity of the HH model allowed a phase-space geometrical analysis of its dynamical properties. In this respect, it is worthwhile to cite the seminal paper of Rinzel and Ermentrout [13]. For a historical perspective, see [12] and [14] (in particular the Introduction).

Some years later, Izhikevich further developed the geometrical analysis of neuronal excitability [15]. The Izhikevich models are characterized by a high biological realism in the generation of several different neural dynamics (such as that of cortical neurons and peripheral receptors), depending on the specific parameter settings and minor variations [2]. Due to this advantage, these models are often used in practical applications where the accurate temporal structure of the generated spike trains is required [6]. The Izhikevich model consists of a system of two differential equations

$$\frac{dv}{dt} = Av^2 + Bv + C - u + \frac{I}{C_r} \quad (1)$$

$$\frac{du}{dt} = a(bv - u) \quad (2)$$

together with an update rule that is applied when the value of the membrane potential  $v$  crosses a pre-defined threshold  $v_{th}$

$$\text{if } v \geq v_{th}, \text{ then } v = c, \quad u = u + d \quad (3)$$

The values  $A = 0.04/(ms \cdot mV)$ ,  $B = 5/ms$  and  $C = 140mV/ms$  are the standard constants of the model; the threshold is set to  $v_{th} = 30mV$ ;  $\frac{I}{C_r}$  represents the input variable ( $mV/ms$ ). The variable  $u$ , referred to as adaptation variable or recovery variable, accounts for the negative feedback on the membrane potential (inactivation of sodium currents and activation of potassium currents).  
 80 The model is very sensitive to the parameters  $(a, b, c, d)$ , tuning which can produce different types of neural dynamics [2].

The ideal continuous-time spike trains from the Izhikevich neuron model were computed for a set of input values by integrating the model equations using the  
 85 Euler method with a small discretization step ( $dt = 1\mu s$ ), for a total duration of  $7000ms$ . A number of spike trains were then computed using 100 different discretization time steps  $dt$  varying logarithmically between  $10\mu s$  and  $10ms$ .

Two sets of parameters were used to simulate different neuron types, corresponding to different regimes of dynamics, using reference values for the  
 90 parameters [2]. Regular spiking (RS) neurons were simulated using parameters  $a = 0.02$ ,  $b = 0.2ms^{-1}$ ,  $c = -65mV$ ,  $d = 8mV$ . Intrinsically bursting (IB) neurons were simulated using parameters  $a = 0.02$ ,  $b = 0.2ms^{-1}$ ,  $c = -55mV$ ,  $d = 4mV$ . The initial values of the variables were set to  $v = c$  and  $u = bv$ , with the corresponding parameter values for each neuron type.

95 The simulations for each neuron type and discretization time step were run with 21 different inputs, taking all the integer values between  $5mV/ms$  and  $25mV/ms$ .

## 2.2. Spike Train Distance Metrics

In this study, the deviation in the temporal structure of the spike sequences  
 100 with respect to an ideal reference spike train was estimated using two different spike distances, the Victor-Purpura distance  $VPd(q)$  [16, 17] and the van Rossum distance  $VRd(\tau)$  [18]. The Victor-Purpura distance is non-Euclidean and event-based, and is computed as the minimum cost required to turn one spike sequence into another using a combination of the following elementary operations:

- 105 • Insertion of a spike (cost= 1)

- Removal of a spike (cost= 1)
- Temporal shift of a spike by an amount of time  $\delta t$  (cost=  $q |\delta t|$ )

where  $q$  represents the relative cost to move a spike and has unit of  $s^{-1}$ . Setting  $q = 0$  means that moving any spike is free of cost. In this case, the distance between two spike trains reduces to the difference in the number of spikes. That is, for  $q = 0$ , the distance is insensitive to the spike position in time. Instead, higher values of  $q$  increasingly penalize shift operations, ultimately making it more expensive than simply removing a spike and inserting it in the correct place (constant cost of 2). The Victor-Purpura distance has been also previously used in the specific context of bionic engineering, for example in bionic touch applications [5, 6].

The van Rossum distance algorithm instead converts the spike trains into continuous functions by convolving each spike train with an exponential kernel (with time constant  $\tau$ ). Then, the distance is computed as an Euclidean integral distance between the two convolved spike trains. In VRd, the  $\tau$  parameter has a similar role as  $1/q$  in VPd. Specifically, low values of  $\tau$  with respect to the inter spike interval make the distance sensitive to the fine temporal differences between the spike trains, while high values of  $\tau$  make it mostly sensitive to the difference in their firing rates.

Finally, a useful measure to characterize the temporal dynamics of spike trains, especially on constant input stimulation, is the average inter-spike interval (ISI), which we compute as

$$ISI = \frac{1}{N-1} \sum_{i=1}^{N-1} (t_{i+1} - t_i) \quad (4)$$

where  $N$  is the number of spikes generated and  $t_i$  are the spike times, sorted in ascending order.

### 2.3. Identification of Limit Discretization Time Steps

Increasing the discretization time step  $dt$  leads to progressively degraded spike trains, due to the increased coarseness of the approximation of the dynamics of the artificial neurons. Two main types of changes can be identified, one due to the progressive build-up of errors in the precise time of each spike, which however preserves the overall structure of the spike train, and another in which the structure of the spike train is completely disrupted, due to too large errors in numeric integration of the model differential equations.

Two different limit discretization time steps can then be defined, one capturing a degree of trade-off between the amount of computation required to simulate the model neurons and the error in the time of each spike (henceforth referred to as  $dt_1$ ), and another reflecting a limit above which the generated spike trains are no longer representative of the ideal, continuous-time dynamics of the models (henceforth referred to as  $dt_2$ ).

The computation of the two limits proposed requires a measure of the quality and correctness of the spike trains produced using different discretization time steps  $dt$  and input values. To do so we proceed as follows. First, for each neuron type and input value we compute a distance matrix using either the Victor-Purpura or van Rossum distances as metric, whose elements correspond to the distance between the reference ideal spike train and spike trains generated with all the combination of values of  $dt$  (rows) and distance-specific parameters (columns; i.e.,  $q$  parameters for VPd and  $\tau$  parameters for VRd). Estimating the distances for multiple values of the parameters is indeed useful, as different parameter values reflect a different weight on the temporal precision of the spike trains, whose exact trade-off may be application-specific. 50 values varying logarithmically between  $0.001/ms$  and  $0.1/ms$  were used for the  $q$  parameters, while the  $\tau$  parameters were set as  $\tau = \frac{1}{q}$ . Thus, for an input of given amplitude, two distance matrices of size  $100 \times 50$  were computed, reflecting different time steps along their rows and different parameter values along their columns.

Then, we use the distance matrices to compute an estimate of the lower and upper limits of the discretization time step  $dt_1$  and  $dt_2$  separately for each value of the distance parameters, using an adaptation of the CUSUM algorithm [19]. CUSUM is a technique that is typically used to detect small cumulative changes in the mean of a signal. Here, we use it to detect significant increases in the spike distances due to increased discretization time steps. Specifically, we compute the upper cumulative sum  $U_i$  by incrementally adding samples  $x(dt_i)$ , computed as explained in the next paragraphs

$$U_i = \begin{cases} 0 & \text{if } i = 1 \\ \max(0, U_{i-1} + x(dt_i) - m - \frac{1}{2}n\sigma) & \text{if } i > 1 \end{cases} \quad (5)$$

where  $m$  and  $\sigma$  are the target mean and standard deviation of the signal, and  $n$  is a mean shift argument that represents the number of standard deviations from the target mean required for change detection. A change point is computed

170 as the first index  $i$  such that  $U_i > c\sigma$ , where  $c$  is the change detection threshold, expressed in target standard deviations of the signal.

The first limit  $dt_1$  is then computed by applying the CUSUM technique to the columns of the distance matrices (i.e., the distances from the reference ideal spike trains as a function of the discretization time step, for each parameter value) to detect a breaking point at which the distance exceeds a target standard deviation of 1 from the ideal target mean of 0 (zero distance, that is, a perfect representation of the spike train with respect to the reference spike train). The set of CUSUM parameters can be tuned to produce more or less conservative estimates of the limit time step. The parameters  $(c, n)$  used in this paper are 175 (10, 10) and (0.2, 0.2) for VPd and VRd on the RS neuron, respectively, and twice their value (20, 20) and (0.4, 0.4) on the IB neuron.

The second limit  $dt_2$  is computed in a similar way, but rather than using the columns of the distance matrices directly, the absolute value of the change in the distance values with increasing  $dt$  is used. CUSUM is then applied similarly as before, with the difference that the target mean value is estimated as the average 185 of the change in distance values for  $dt$  lower than  $0.1ms$ , rather than using the ideal null value. This was done to improve the stability of the system. The parameters used for the detection of the second limit are (40, 40) and (1.5, 1.5) for VPd and VRd on the RS neuron, respectively, and (30, 30) and (0.7, 0.7) for the IB neuron.

190 Specific values of  $dt_1$  and  $dt_2$  (for each distance parameter value) were computed for all the input amplitudes used ( $5mV/ms$  to  $25mV/ms$ ), for both neuron types (RS and IB), and for both distance metrics (VPd and VRd).

### 3. Results

195 The spike trains computed as a function of all the different discretization time steps are shown in Figure 2 (left) as raster plots. The first row shows the results for the RS neuron model, while the bottom row shows the results for the IB neuron model. Figure 2 (middle-right) shows the distance matrices computed using the Victor-Purpura (VPd) and van Rossum (VRd) distances. The distance matrices report the value of the distance between the reference ideal spike train and spike trains computed using different discretization time steps (rows), and a range of parameters for the distance functions (columns, corresponding to  $q$  values for VPd and  $\tau$  values for VRd). The upper and lower limit time steps are marked with thick white lines as a function of the distance parameters, showing 200



205 how different parameters that prioritize different aspects of the approximated spike trains can have a significant effect on the resulting lower limit.

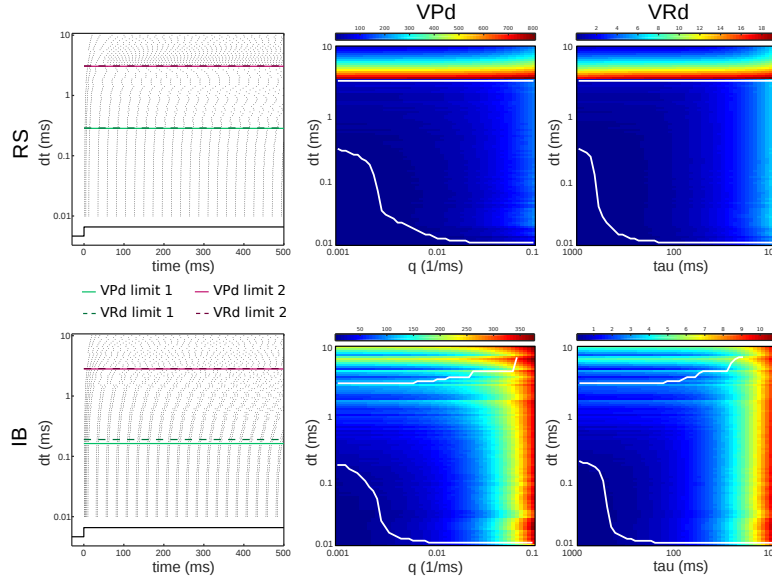


Figure 2: The raster plots on the left show the firing activity of a regular spiking (RS; top) and intrinsically bursting (IB; bottom) Izhikevich neuron model computed using a fixed input of  $20mV/ms$  and different discretization time steps ( $dt$ ). Limit discretization time steps  $dt_1$  and  $dt_2$  are shown in overlay, computed using both VPd and VRd distances and a fixed parameter value of  $q = 0.001/ms$  for VPd and  $\tau = 1000ms$  for VRd. The other panels at the right of the raster plots show the distance matrices computed using the Victor-Purpura (VPd; middle column) and van Rossum (VRd; right column) distances for every combination of discretization time step ( $dt$ ) and parameter value ( $q$  for VPd, and  $\tau = \frac{1}{q}$  for VRd). The computed limit discretization time steps  $dt_1$  and  $dt_2$  are shown in overlay as white lines, as a function of the parameters of the distance functions.

The two limit time steps implicitly define three regions over the range of time steps, exhibiting different dynamics. For time steps lower than  $dt_1$ , the generated spike trains closely resemble the target, ideal spike train. For higher time steps, 210 the spike trains progressively degrade in quality, until they completely lose their structure when approaching  $dt_2$ .

The dynamics of the generated spike trains in the three regions can be understood by inspection of the  $u$ - $v$  space, as is shown in Figure 3. Specifically, increasing the discretization time step introduces small errors in the dynamics 215 of the system due to “overshooting” of the membrane potential  $v$ , that lead to irregular spikes and temporal errors that build-up over time. Ultimately, time steps higher than the upper limit  $dt_2$  result in a complete loss of the structure of the spike trains.

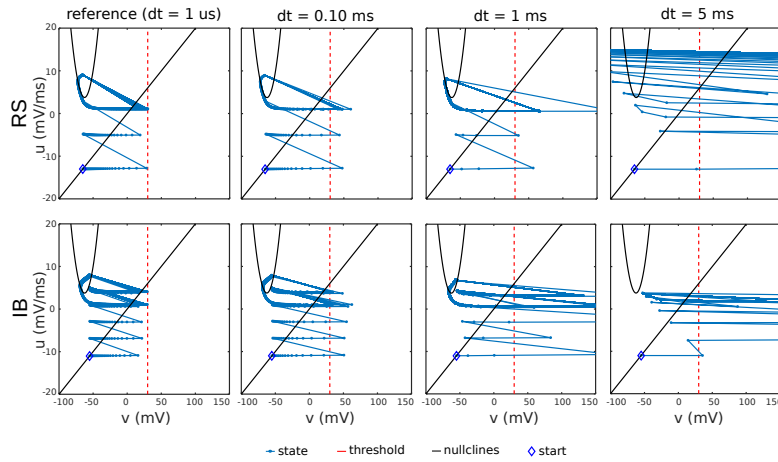


Figure 3: The trace of the model variables is shown in the  $u-v$  phase space for a regular spiking (RS; top) and intrinsically bursting (IB; bottom) Izhikevich neuron model. The dynamics were computed using a fixed input of  $25\text{mV/ms}$  and three values of the discretization time step ( $0.1\text{ms}$ ,  $1\text{ms}$ ,  $5\text{ms}$ ), along with an ideal reference trace computed using  $dt = 1\mu\text{s}$ . Note that as in Fig. 1, the value of the membrane potential  $v$  can exceed the threshold of  $30\text{mV}$  if the single update that leads to its crossing is very large, for example when using large time steps.

We further explored the computed limit discretization time steps over a full  
 220 range of input amplitudes, which produce spike trains with different structure  
 (Figures 4 and 5). In particular, increasing the input amplitude increases the  
 firing rate of the neurons, thereby reducing the average inter-spike interval (ISI).

The behaviour of the lower limit  $dt_1$  was found to be highly consistent for  
 both neuron types and is characterised by a clear decrease with increasing input  
 225 values. As increased input values are observed to produce decreasing inter-spike  
 intervals (ISI; middle column of Fig. 6), we further analysed the relationship  
 between the limit  $dt_1$  and the ISI directly (Fig. 6, third column), finding a linear  
 relation between the two variables in the range considered.

It is interesting to observe that while the upper limit  $dt_2$  was found to be of  
 230 the order of  $3\text{ms}$ , with low variation depending on the input, in the RS neuron,  
 its behaviour as a function of the input seems to be less obvious in the IB neuron,  
 as shown in Fig. 6 (first column). This is however not surprising as inspection  
 of the raster plots of the IB neuron shows a generally smoother break-down in  
 the structure of the generated spike trains with increased time steps, contrary  
 235 to the clear and disruptive effect on the RS neuron (see Figures 2, 4 and 5).

We then finally extended the analysis of Fig. 6, which is based on a single  
 value of  $q$  (for VPd) and  $\tau$  (VRd), to explore the stability of the strength of the

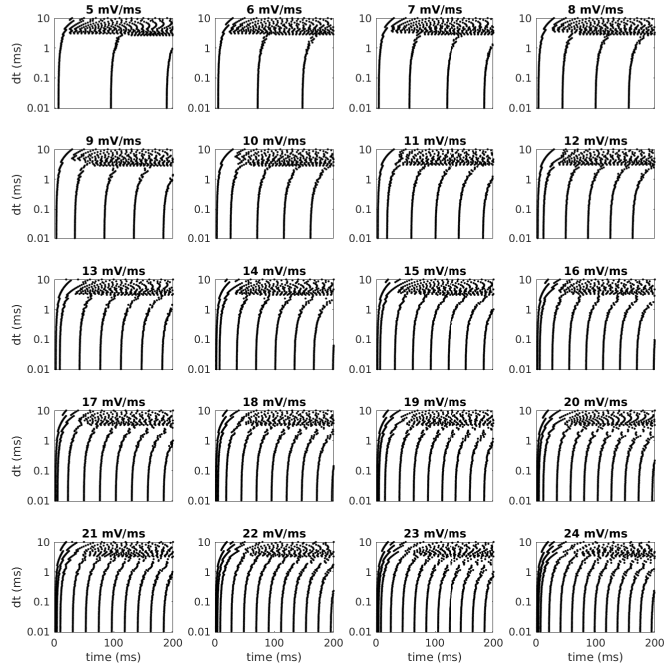


Figure 4: Full set of raster plots for the regular spiking (RS) Izhikevich artificial neuron used in the main paper, for a range of input values from  $5mV/ms$  to  $24mV/ms$ .

linear relation between the limit  $dt_1$  and the ISI while varying the parameters of the distance function. The results are reported in Fig. 7. We observe that  
 240 for low values of  $q$  (and corresponding high values of  $\tau = \frac{1}{q}$ ) the strength of the linear relation is stable and approximately constant; higher values of the parameters, however, produce a sharp change in regime until finally  $dt_1$  becomes almost independent from the ISI.

#### 4. Discussion and conclusion

245 The application in bionic engineering and neuro-robotics of artificial neuron models that use Euler integration requires the explicit choice of a discretization time step to achieve a trade-off between the amount of computation required for the simulation of the neurons and the fidelity of their generated behaviour with respect to an ideal, continuous-time solution. The Izhikevich neuron model  
 250 has been previously identified as a good candidate for this scope, due to its

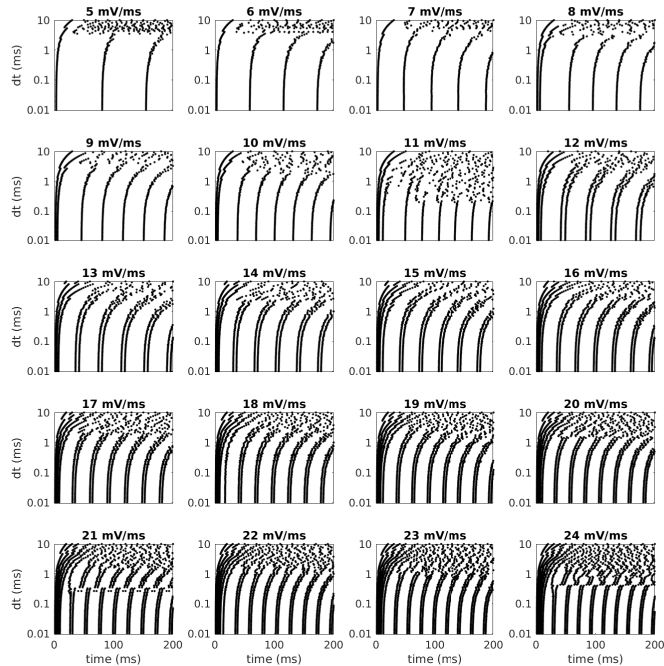


Figure 5: Full set of raster plots for the intrinsically bursting (IB) Izhikevich artificial neuron used in the main paper, for a range of input values from  $5mV/ms$  to  $24mV/ms$ .

capacity to reproduce a large variety of dynamics of biological neurons while only requiring 13 floating point operations per update [3, 1]. The total number of FLOPS (floating-point operations per second) required to simulate a single neuron in real-time using a discretization time step  $dt$  is thus  $\frac{13}{dt}$ , or alternatively  
 255 the total number of artificial neurons that can be simulated on a computer system capable of  $P$  (measured in FLOPS) is  $N = \frac{P \cdot dt}{13}$ . Thus, the use of larger time steps allows for the simulation of a significantly larger number of artificial neurons in real-time, on the same platform. Note that this relation on  $dt$  is valid

260 In this work, we explored the effect of the discretization time step on the quality of the spike trains generated using the Izhikevich neuron model under regular spiking (RS) and intrinsically bursting (IB) dynamics, evaluated with step inputs of various amplitudes. The degree of convergence of the models was measured using the distance between the spike trains produced with an

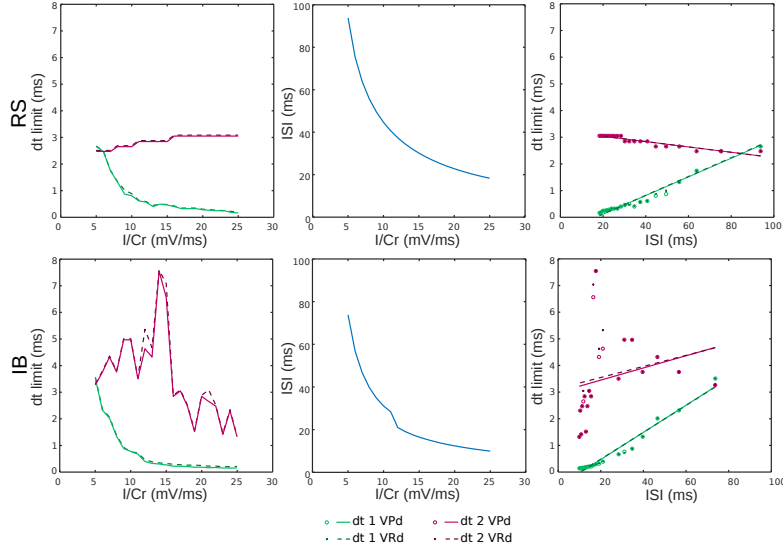


Figure 6: The figure shows the limit discretization time steps computed using the Victor-Purpura (VPd; red) and van Rossum (VRd; green) distances as a function of the input value used (left column) and of the average inter-spike interval (ISI; right column), using a fixed parameter value of  $q = 0.001ms^{-1}$ ,  $\tau = \frac{1}{q} = 1000ms$ . The right column further shows a linear fitting of the data ( $y = ax + b$ ) to compute the slope of change in the value of the limit  $dt$  as a function of the ISI to different inputs. The coefficient of the fitted lines for the RS neuron are 0.035 for  $dt_1$  and  $-0.01$  for  $dt_2$ , regardless of the distance metric used, while for the IB neuron are 0.051 and 0.05 for  $dt_1$ , Victor-Purpura and van Rossum, respectively, and 0.035 for  $dt_2$  for both distances. The middle column shows the relation between the input value and the average inter-spike interval. Results are reported for a regular spiking (RS; top) and intrinsically bursting (IB) Izhikevich neuron model.

265 ideal  $dt = 1\mu s$ , approximating a continuous-time exact solution of the system, and spike trains produced with increasing values of  $dt$ . Two distance metrics were compared in parallel, Victor-Purpura and van Rossum, so to evaluate the generality of the proposed approach.

Specifically, we found that two limits can be defined, a lower limit  $dt_1$  270 reflecting the build-up of errors in the timing of the individual generated spikes, which however still retain the large-scale structure of the spike train, and an upper limit  $dt_2$  above which numeric integration fails and any input-specific structure is lost.

The  $dt_1$  limit was found to have a strong dependency on the average ISI on 275 both neuron types, and to increase with increasing ISI values. In particular, it was found that spike trains with high ISI, that is low average firing rate, could be accurately simulated using large time steps ( $dt \in [1ms, 2ms]$ ), though spike trains with low ISI (high average firing rate), which are more common in practical

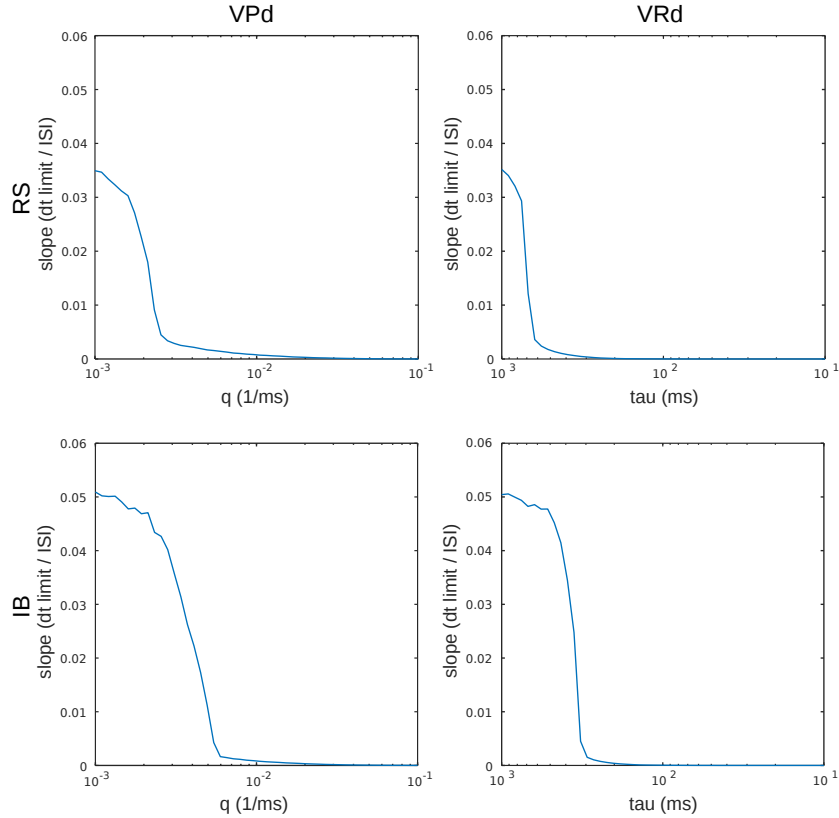


Figure 7: Investigation of the effect of the distance parameters ( $q$  and  $\tau$ ) on the estimated slope of the linear relation between the  $dt_1$  limit and the average ISI (Fig. 6, right column). The  $dt_1$  limit was found to depend linearly on the average ISI for low values of the  $q$  parameter (and equivalently, for high values of the  $\tau$  parameter), while it was found to be independent from it for higher values.

applications, were found to require smaller time steps ( $dt \in [0.1ms, 1ms]$ ). It  
 280 is thus important to stress that the exact value of the limit discretization time  
 step depends on the expected magnitude of the inputs, which is reflected in the  
 firing rate and ISI of the neuron model. The relation between the  $dt_1$  limit and  
 the average ISI was found to be approximately linear within the range of input  
 values considered, that introduces a sort of Nyquist-like criterion suggesting  
 285 a lower-limit discretization as a function of the ISI and the desired temporal  
 precision (which is reflected in the choice of  $q$  or  $\tau$  parameters and in the CUSUM  
 coefficients). For example, using the present CUSUM parameters and the the  
 values of  $q$  and  $\tau$  used in Fig. 2 and Fig. 6 ( $q = 0.001/ms$ ,  $\tau = 1000ms$ ), a

Nyquist-like criterion can be formulated suggesting a sampling frequency around  
290  $\frac{30}{\text{ISI}}$  for RS and  $\frac{20}{\text{ISI}}$  for IB.

The  $dt_2$  limit was found to be well defined in the regular spiking model, and decreasing with the average ISI. However, its estimate was less clear in the intrinsically bursting model, and not always clear even from visual inspection of the spike trains (see Figures 2, 4 and 5). Nonetheless, it was found that  $dt_2$   
295 was always larger than  $2 - 3ms$ , which can thus be used as an approximate upper bound for the discretization time step in any application using Izhikevich neurons.

Finally, investigation of the effect of the parameters of the distance metrics ( $q$  and  $\tau$ ) on the slope of the linear relation between the  $dt_1$  limit and the average  
300 ISI found that the strength of the relation is stable and approximately constant for a range of values (small  $q$ , high  $\tau$ ), but disappears for others (zero slope, fairly constant  $dt_1$  regardless of the average ISI; high  $q$ , small  $\tau$ ). This is easily explained by the fact that high values of  $q$  (low values of  $\tau$ ) enforce stricter requirements on the exact timing of the individual spikes, and thus require small  
305 values of  $dt$  for an accurate representation of the spike train.

The actual value of the  $dt_1$  limit thus depends on the degree of accuracy that specific applications may require, and that can be incorporated in the choice of the parameters of the distance metrics used and in the parameters of the CUSUM algorithm, allowing for more or less strict estimates of the limit.

Indeed, contrary to previous work [10] that tried to identify a single limit  
310 discretization time step that guaranteed almost exact dynamics, here we were interested in finding broad ranges of time steps to allow for a trade-off between the temporal precision of the produced spike trains and the computational requirements necessary to produce them. Specifically, we determined three  
315 different regimes as a function of the time step  $dt$ , 1) guaranteeing high accuracy of the generated spike trains ( $dt < dt_1$ ), 2) trading off a lower accuracy in exchange for lower computational requirements ( $dt_1 < dt < dt_2$ ), and 3) ultimately breaking up the structure of the desired spike trains ( $dt > dt_2$ ).

The algorithms we presented to compute the  $dt_1$  and  $dt_2$  limits can be further  
320 extended to other neuron models that were not used here (e.g., Integrate & Fire, ...) and other neuron types (e.g., Chattering CH, ...). The results were also found to be robust regardless the distance metrics used, Victor-Purpura and van Rossum, and fairly consistent between them. It is thus likely that other metrics may be used for specific applications, depending on their individual requirements  
325 [20], for example where sensitivity to bursts and silent periods is desired [21].

In conclusion, we have analyzed the errors introduced by using large discretization time steps to simulate Izhikevich artificial neurons using the Euler integration method. In particular, we presented a novel method to estimate two discretization limits and we discussed how they can be used to choose an optimal value of time step to reflect a trade-off between the amount of computation required and the quality of the simulated spike trains.

### Conflict of Interest Statement

CMO and GS have a patent related to this study, titled “Method and apparatus for transmitting tactile sensations to an user” (Italian patent number 0001417070).

### Author Contributions

HG and GS implemented the discretized Izhikevich model, performed data analysis, discussed the results and wrote the paper; AM designed and performed part of the data analysis, discussed the results and wrote the paper; EC contributed to data analysis, discussed the results and wrote the paper; CMO designed and supervised the study, contributed to data analysis, discussed the results and wrote the paper.

### Acknowledgments

The authors thank Prof. Maria Chiara Carrozza, Prof. Paolo Dario and Prof. Silvestro Micera for their seminal research in neuro-robotics and for collaborations towards neuroengineering applications and Prof. Henrik Jøntell and Prof. Johan Wessberg for discussions about neurophysiology. This study was partially funded by the EU Grant FET 611687 NEBIAS project (Neurocontrolled Bidirectional Artificial upper limb and hand prosthesis), by the Italian Ministry of Education, Universities and Research via the Italy-Sweden bilateral research project J52I15000030005 SensBrain (Brain network mechanisms for integration of natural tactile input patterns), and by the National Institute for Insurance against Accidents at Work (INAIL) via the MOTU project.

[1] G. Spigler, C. M. Oddo, M. C. Carrozza, Soft-neuromorphic artificial touch for applications in neuro-robotics, in: Biomedical Robotics and Biomechatronics (BioRob), 2012 4th IEEE RAS & EMBS International Conference on, IEEE, 2012, pp. 1913–1918.



- [2] E. M. Izhikevich, Simple model of spiking neurons, *IEEE Transactions on neural networks* 14 (6) (2003) 1569–1572.
- 360 [3] E. M. Izhikevich, Which model to use for cortical spiking neurons?, *IEEE Transactions on Neural Networks* 15 (5) (2004) 1063–1070. doi:10.1109/TNN.2004.832719.
- [4] M. Ambroise, T. Levi, S. Joucla, B. Yvert, S. Saghi, Real-time biomimetic central pattern generators in an fpga for hybrid experiments, *Frontiers in Neuroscience* 7 (2013) 215. doi:10.3389/fnins.2013.00215.  
365 URL <http://journal.frontiersin.org/article/10.3389/fnins.2013.00215>
- [5] U. B. Rongala, A. Mazzoni, C. M. Oddo, Neuromorphic artificial touch for categorization of naturalistic textures, *IEEE transactions on neural networks and learning systems* 28 (4) (2017) 819–829.  
370
- [6] C. M. Oddo, S. Raspopovic, F. Artoni, A. Mazzoni, G. Spigler, F. Petrini, F. Giambattistelli, F. Vecchio, F. Miraglia, L. Zollo, G. D. Pino, D. Camboni, M. C. Carrozza, E. Guglielmelli, P. M. Rossini, U. Faraguna, S. Micera, Intraneural stimulation elicits discrimination of textural features by artificial fingertip in intact and amputee humans, *eLife* doi:<http://dx.doi.org/10.7554/eLife.09148>.  
375
- [7] M. D. Humphries, K. N. Gurney, Solution methods for a new class of simple model neurons, *Neural Computation* 19 (12) (2007) 3216–3225. doi:10.1162/neco.2007.19.12.3216.  
380 URL <http://dx.doi.org/10.1162/neco.2007.19.12.3216>
- [8] L. N. Long, G. Fang, A review of biologically plausible neuron models for spiking neural networks, in: *AIAA Infotech@Aerospace Conference and Exhibit*, Vol. 2,548 (3 Vols), American Institute for Aeronautics and Astronautics ( AIAA ), 2010.
- 385 [9] M. Hopkins, S. Furber, Accuracy and efficiency in fixed-point neural ode solvers, *Neural Computation* 27 (10) (2015) 2148–2182. doi:10.1162/NECO\_a\_00772.
- [10] M. J. Skocik, L. N. Long, On the capabilities and computational costs of neuron models, *IEEE Transactions on neural networks and learning systems* 25 (8) (2014) 1474–1483.  
390

- [11] H. A. Hodgkin AL, A quantitative description of membrane current and its application to conduction and excitation in nerve, *The Journal of Physiology* (117(4)) (1952) 500–544.
- [12] J. Rinzel, Discussion: Electrical excitability of cells, theory and experiment: Review of the hodgkin-huxley foundation and an update, *Bulletin of Mathematical Biology* 52 (1-2) (1990) 5–23.
- [13] J. Rinzel, G. B. Ermentrout, Analysis of neural excitability and oscillations, *Methods in neuronal modeling: From ions to networks* 2 (1998) 251–291.
- [14] E. M. Izhikevich, *Dynamical systems in neuroscience*, MIT press, 2007.
- [15] E. M. Izhikevich, Neural excitability, spiking and bursting, *International Journal of Bifurcation and Chaos* 10 (06) (2000) 1171–1266.
- [16] Victor, Purpura, Nature and precision of temporal coding in visual cortex: a metric-space analysis, *Journal of Neurophysiology* 76 (2) (1996) 1310–1326.
- [17] J. D. Victor, K. P. Purpura, Metric-space analysis of spike trains: theory, algorithms and application, *Network: Computation in Neural Systems* 8 (2) (1997) 127–164. doi:10.1088/0954-898X\8\2\003.
- [18] M. C. van Rossum, A novel spike distance, *Neural computation* 13 (4) (2001) 751–763.
- [19] E. S. Page, Continuous inspection schemes, *Biometrika* 41 (1/2) (1954) 100–115.
- [20] E. Satuvuori, T. Kreuz, Which spike train distance is most suitable for distinguishing rate and temporal coding?, *arXiv preprint arXiv:1708.07508*.
- [21] D. Lyttle, J.-M. Fellous, A new similarity measure for spike trains: sensitivity to bursts and periods of inhibition, *Journal of neuroscience methods* 199 (2) (2011) 296–309.